

Central peak position in magnetization hysteresis loops of ferromagnet/superconductor/ferromagnet trilayered films

S. Kobayashi,^{1,*} H. Oike,² M. Takeda,³ and F. Itoh²

¹*Satellite Venture Business Laboratory, Gunma University, 1-5-1 Tenjin-cho, Kiryu, Gunma 376-8515, Japan*

²*Department of Electronic Engineering, Gunma University, 1-5-1 Tenjin-cho, Kiryu, Gunma 376-8515, Japan*

³*Physics Department, Graduate School of Science, Tohoku University, Aramaki Aoba-ku, Sendai, 980-8578, Japan*

(Received 8 August 2002; published 27 December 2002)

We report on the magnetization hysteresis loops of rf-sputtered Co/Nb/Co trilayered films under applied fields parallel to the film surface. Below superconducting transition temperature T_c , the central peak around zero field in the superconducting magnetization is found to be anomalously shifted toward a positive field on the descending branch of the hysteresis loop, in contrast to a negative peak position of a single superconducting film observed in this geometry. The central magnetization peak shifts toward a lower field with decreasing temperature and increasing the thickness of superconducting Nb layer. These results are explained as due to the stray field of the ferromagnetic Co layer with in-plane magnetization, which effectively reduces the internal field of the superconductor.

DOI: 10.1103/PhysRevB.66.214520

PACS number(s): 74.80.Dm, 74.25.Ha

I. INTRODUCTION

The magnetization hysteresis loop, which is related to the field dependence of the critical current density, is important for applications and is widely used to characterize superconducting materials. These properties reflect the internal-field profile of superconductors which is created by the screening field, trapped flux, demagnetizing field, etc.¹ The field dependence of the internal field and therefore, the shape of the hysteresis loop can be modified in a controlled way by changing the sample geometry and microstructure of sample and by introducing artificial defects.

Recently, much attention has been paid to the influence of the magnetic field of ferromagnets on the superconducting bulk properties in ferromagnet/superconductor (F/S) heterostructures. Since the ferromagnet produces the stray field, the internal field of the superconductor in contact with a ferromagnet is strongly modified and bulk properties absent in a single superconductor would be induced. For instance, in the regular arrays of magnetic dots covered by a type-II superconducting film under a perpendicular applied field, the internal field of the superconductor is locally modified around the ferromagnetic dots and the penetrating vortices are magnetically pinned. This pinning effect results in a pronounced commensurability effect and asymmetry in the magnetization hysteresis loops which depend on the relative alignment between the ferromagnet magnetization and vortices.² On the one hand, in a mesoscopic F/S nanostructure including F/S junctions, anomalies in the magnetoresistance implying the reentrance of the superconductor to the normal state were observed under perpendicular³ and parallel⁴ applied fields. These anomalies were qualitatively explained by the pair-breaking effect due to Zeeman splitting, whose characteristic field is given by the summation of the applied field and stray field of the ferromagnet with in-plane magnetization.

In this paper, we report on the results of magnetization measurements on ferromagnet(Co)/superconductor(Nb)/ferromagnet(Co) trilayered films under applied fields parallel

to the film surface. Although there have been some reports concerning the magnetization hysteresis loops of F/S layered systems under a parallel field orientation,^{5,6} the influence of the ferromagnet magnetization on the superconducting magnetization was not discussed in detail. We show that when the system has a layered structure and the ferromagnet has in-plane magnetization, the central peak of the superconducting magnetization is significantly shifted from a negative field toward a positive field on the descending branch of the hysteresis loop. The qualitative explanation is given in view of the internal field of the superconductor which is a summation of the applied field and the stray field of the ferromagnetic layer.

II. EXPERIMENT

The Co/Nb/Co trilayers were prepared at room temperature on Si(100) substrates using a rf-sputtering system with a rotatable substrate holder. The Nb and Co sputtering targets were 99.95% and 99.99% in purity, respectively. The base pressure was less than 2×10^{-7} Torr. To achieve a high superconducting transition temperature T_c , the Nb layer was deposited with a high sputtering rate under Ar pressure of 30 mTorr; the sputtering rate of Nb and Co was 5.7 Å/sec and 5.6 Å/sec, respectively. The layer thickness of Co and Nb is $d_{\text{Co}} = 200, 500$ Å and $d_{\text{Nb}} = 500 - 2000$ Å. To avoid surface oxidation, a 50-Å Nb capping layer was deposited on top of the film. We also prepared a multilayered sample with $d_{\text{Co}} = 500$ Å and $d_{\text{Nb}} = 1000$ Å where the number of Co/Nb bilayers is 5. The Co/Nb multilayer exhibited the same superconducting properties as that of the trilayer with equal sublayer thickness and was used for structural characterization. For a reference film, a single Nb film with thickness of 2500 Å was prepared. The samples fabricated in the present study are listed in Table I.

Figure 1(a) shows a typical high-angle x-ray diffraction spectrum of the multilayered sample, i.e., M-Co1, taken at room temperature by a θ - 2θ scan with Cu $K\alpha$ radiation. Several Bragg reflections due to the bcc structure of Nb were

TABLE I. The prepared samples and their superconducting transition temperatures. M , T , and S in sample name represent multilayer, trilayer, and single films, respectively.

Sample	d_{Nb} (Å)	d_{Co} (Å)	T_c (K)
M -Co1	1000	500	7.8
T -Co1	500	200	6.2
T -Co2	750	200	6.3
T -Co3	1000	500	7.8
T -Co4	2000	500	8.2
S -Nb	2500		8.5

observed, being indicative of the polycrystalline nature of the sample with no preferred orientation. On the other hand, for the Co layer, two Bragg reflections were observed at $2\theta = 43.9^\circ$ and 97.7° , which can be assigned as hcp (002) or fcc (111) and hcp (004) or fcc (222), respectively. These two reflections appeared even in the 2θ scan with arbitrary x-ray incident angle to the film plane. Therefore, the Co layer

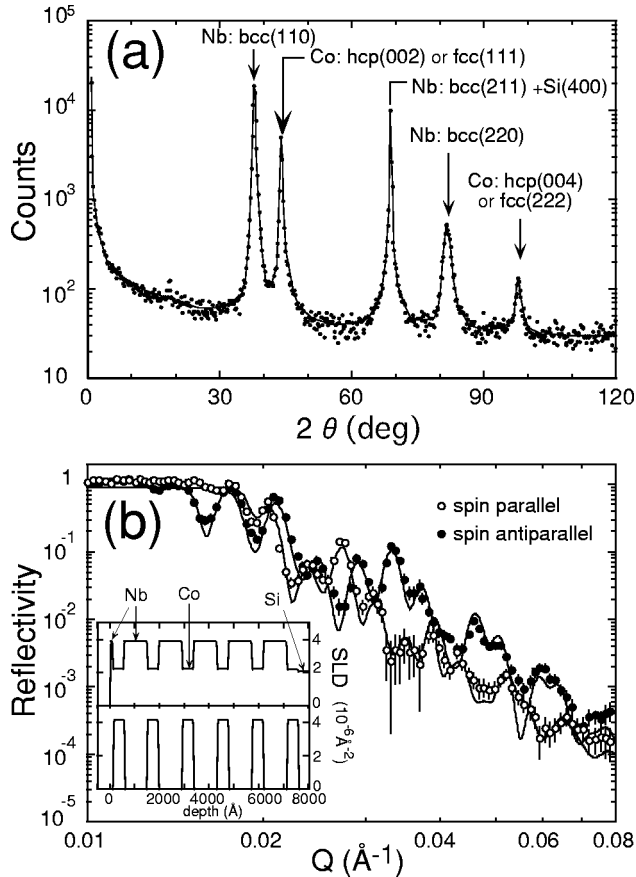


FIG. 1. (a) High-angle x-ray diffraction profile of the M -Co1 sample, taken at room temperature. (b) Specular polarized neutron reflectivity of the M -Co1 sample, taken at $T=12$ K and $H=1$ kOe. The open and solid circles show the data for neutrons with spin parallel and antiparallel to H , respectively. The upper and lower panels in the inset show the nuclear and magnetic scattering length density profiles, respectively, obtained by least-squares fittings.

would be polycrystalline where the hcp planes are randomly stacked along the hexagonal c axis within grains.

In order to confirm the layered structure of sample, we performed specular polarized neutron reflectivity (SPNR) measurements on the M -Co1 sample, using a PORE reflectometer,⁷ installed at KENS, Neutron Science Laboratory in High Energy Accelerator Research Organization (KEK), in Tsukuba, Japan. The SPNR measurements give information about the depth profile of both magnetic and nuclear scattering length densities (SLD) along the direction perpendicular to the film plane. Measurements were performed at $T=12$ K above T_c under an applied field of 1 kOe parallel to the film plane, which is enough to saturate the magnetic Co moments. Figure 1(b) shows the SPNR for neutron spins parallel and antiparallel to the applied field H . The dependence of the SPNR on the neutron polarization is due to the in-plane magnetization of the Co layer. Assuming that each Co (or Nb) layer has an equal layer thickness and has uniform magnetic and nuclear SLD, the least-squares fits yielded the depth profile of the SLD as shown in the inset of Fig. 1(b). Good fits to the observed data confirmed the layered structure of the sample. The error of the sublayer thickness was within 10% of the designed value and the root-mean-square roughness parameter was typically 40 Å in our samples.

The superconducting transition temperatures T_c at zero field and upper critical fields were determined by conventional four-probe resistivity measurements, by varying the temperature under constant applied field. The transition temperature was defined as the temperature where the sample resistance becomes half that just above the transition. All samples showed a sharp superconducting transition with a transition width of 0.1 K (10%–90%). From the upper critical fields, the Ginzburg-Landau coherence length ξ and the London penetration depth λ at $T=0$ K of our samples were found, in the dirty limit, to be 105 Å and 630 Å, respectively.

The magnetization under applied fields parallel to the film plane was measured with a superconducting quantum interference device (SQUID) magnetometer (Quantum Design MPMS-5S). The measurements were performed in the reciprocating sample (RSO) mode in the center scan with a frequency of 1 Hz and an amplitude of 3 cm. The lateral dimension of the sample was typically 2×2 mm². The applied field was changed with “no overshoot mode.” To remove the field inhomogeneity of the superconducting magnet which produces artifacts, the applied field was set to zero field with an oscillating field with decreasing amplitude and then the magnet was quenched before the measurements. We also monitored the raw SQUID voltage data to ensure the reliability of the observed data. All hysteresis loops below T_c were recorded after zero-field cooling (ZFC) with a positively magnetized Co state; this state was produced by applying a field of +0.5 kOe before quenching the magnet.

III. RESULTS AND DISCUSSION

As a typical example, Fig. 2 shows the magnetization hysteresis loops of the T -Co2 sample, taken at a temperature above and below T_c . At $T=10$ K above T_c , the hysteresis

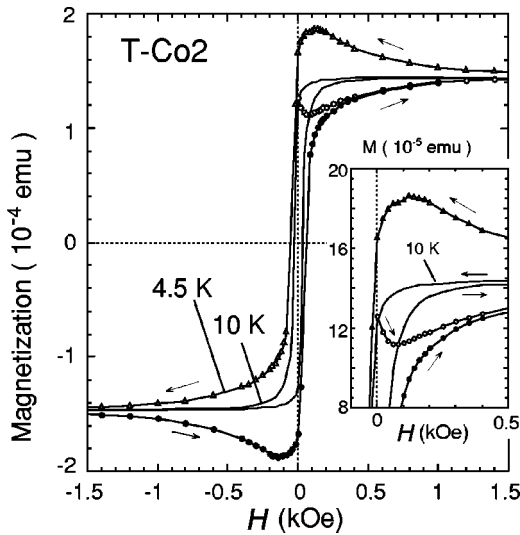


FIG. 2. Magnetization hysteresis loops of the *T-Co2* sample, measured after ZFC. The inset shows the enlargement around zero applied field. The open circles, triangles, and solid circles represent the data, taken on increasing the field after ZFC, on decreasing the field from + 4 kOe, and on increasing the field from - 4 kOe, respectively.

loop is typical of a ferromagnetic film with in-plane anisotropy and has a coercive field of about 50 Oe. On cooling the samples below T_c , the superconducting signal is added on the hysteresis loop at $T=10$ K for all samples investigated. As can be seen in the inset of Fig. 2, with increasing the applied field after ZFC the magnetization shows the usual diamagnetic behavior and then increases toward the value at $T=10$ K. On decreasing the field from a high field, the magnetization increases due to vortex pinning and then shows a maximum around $H=100$ Oe, followed by a sharp reduction compared with the magnetization reduction at $T=10$ K.

To show clearly the superconducting signal of Nb, the magnetization at $T=10$ K is subtracted from the data below T_c as shown in Fig. 3. Note that from magnetization measurements at $T=10$ K after heating at an arbitrary field on the descending branch of the hysteresis loop below T_c , we found that the hysteresis loop of the ferromagnet magnetization below T_c is slightly modified at fields very close to the coercive field where the magnetic susceptibility maximizes. This might be due to the reshuffling of magnetic domains in the ferromagnet by the magnetic field created by pinned vortices or by screening effects of the stray field.⁸ Therefore, the data around the coercive field were omitted from the figures.

As shown in Fig. 3(a), for *T-Co2* with $d_{Nb}=750$ Å, the central peak around zero field in the superconducting magnetization was found to be anomalously shifted toward a positive field on the descending branch of the hysteresis loop while it shifted toward a negative field on the ascending one. With decreasing temperature, the central peak position gradually shifts toward zero field. This behavior is sharply in contrast to the hysteresis loop of the single Nb film *S-Nb* in this geometry shown in Fig. 3(b), where the central peak is located at zero field just below T_c and shifts toward a further negative field at low temperatures.

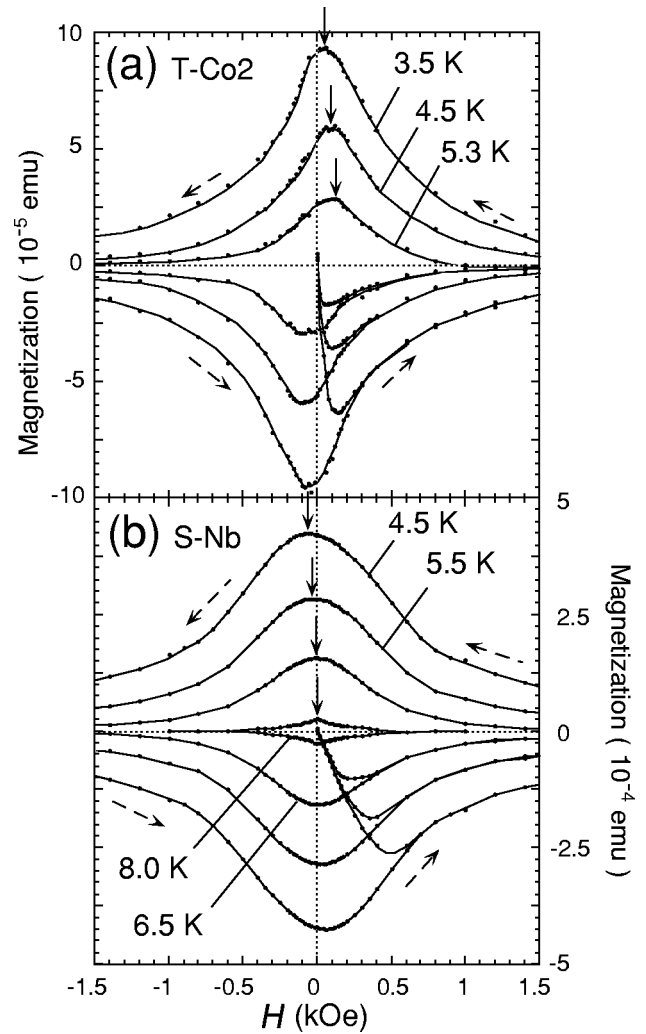


FIG. 3. Hysteresis loops of superconducting magnetization for (a) *T-Co2* and (b) *S-Nb* at various temperatures, where the magnetization at $T=10$ K is subtracted. The solid arrows indicate the position of the central magnetization peak.

The temperature variation of the central peak position H_{pM} obtained on the descending branch of the hysteresis loops is shown in Fig. 4. For all trilayered samples, H_{pM} is about 200 Oe just below T_c and shifts toward a lower field with decreasing temperature. Even at the lowest measuring temperature, a negative peak position was not detected when d_{Nb} is small, while H_{pM} rapidly crosses the zero field and shifts toward a further negative field in the case of large d_{Nb} . Particularly, for *T-Co4* with $d_{Nb}=2000$ Å, H_{pM} below $T/T_c \sim 0.7$ almost coincides with that of *S-Nb*, indicating that the influence of the ferromagnet is ineffective in this case.

Generally, superconductors show a central magnetization peak at a negative field on the descending branch of the hysteresis loop due to the field-dependent critical current density. At the field where the central peak appears, the mean internal field throughout the superconducting specimen is minimum so that the current density which contributes to the total magnetic moment maximizes. Within the context of the critical-state model taking account of the field-dependent critical current density, the central magnetization peak of the

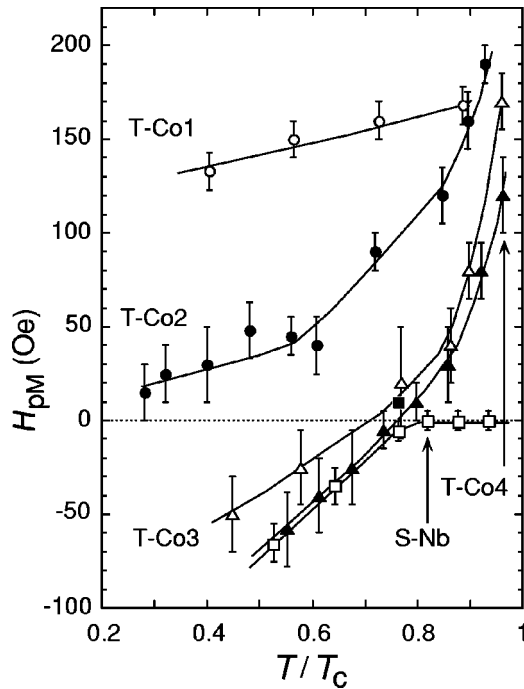


FIG. 4. Temperature variation of the central peak position, obtained on the descending branch of the hysteresis loop: T-Co1 (open circles), T-Co2 (solid circles), T-Co3 (open triangles), T-Co4 (solid triangles), and S-Nb (squares). Solid lines are guides to eyes.

rectangular slab (i.e., the thick film with thickness much larger than the London penetration depth λ) under applied fields parallel to the surface is always located at a negative field on the descending branch of the hysteresis loop.^{9,10} This arises from the fact that the internal field of the great majority of the superconducting region is delayed behind the applied field and a large positive internal field remains in the remanent state when reducing the applied field from a high field.

On the other hand, when the film thickness is comparable with λ , the superconductor is magnetically transparent and the internal field is sensitive to the sweeping applied field. As a consequence, reconstruction of the internal field can be quickly achieved over the entire sample if the direction of the applied field is varied. Then, the central magnetization peak appears at a slightly negative field or even at zero applied field. This behavior is clearly seen in the central peak position of the S-Nb sample shown in Figs. 3(b) and 4.

When a superconducting film is in contact with a ferromagnetic layer with in-plane magnetization, however, the central peak position will be changed dramatically. Since the ferromagnet produces a stray field along the surface antiparallel to its in-plane magnetization, the internal field of the superconductor is modified. Particularly, when a field positive enough to saturate the ferromagnet magnetization is applied, the stray field is antiparallel to the applied field and the internal field is effectively reduced. Therefore, the condition that the mean internal field minimizes can be achieved even at a *positive* field. This results in a positive H_{pM} on the descending branch of the hysteresis loop as shown in Fig. 4. At sufficiently high temperatures where the field penetration

into the superconductor is very large, the mean internal field is less dependent on the film thickness, yielding nearly the same $H_{pM} \sim 200$ Oe for all trilayers investigated. This value roughly corresponds to the strength of the effective stray field acting on the superconductor in this geometry and is in good agreement with that determined from our recent transport critical current measurements.¹¹ When lowering the temperature, however, the field penetration is suppressed and a positive internal field develops locally around the center of the film in the remanent state. This results in a shift of H_{pM} toward a lower field at low temperatures as shown in Fig. 4. Note that within the experimental accuracy no pronounced anomaly in the superconducting magnetization was detected around the coercive field where the direction of the effective stray field is reversed.

From simple analytical calculations, the stray field around a ferromagnetic film with in-plane magnetization and flat surface was determined. It was found that while the stray field is very large ($> 10^3$ Oe) around the edge of the superconducting film (near the poles of the ferromagnet), the stray field that almost the majority of the superconducting region feels is only of the order of a few Oe. This value is small compared with the effective stray field of 200 Oe, obtained from H_{pM} at high temperatures. The existing large interfacial roughness might modify the distribution of the stray field around the F/S interface and increase the effective stray field inside the superconductor. Theoretical works are necessary to quantitatively explain the position of the central magnetization peak in F/S-layered systems including ferromagnets with in-plane magnetization.

Finally, it should be noted that a positive central peak position has been observed also in granular high- T_c superconducting films under perpendicular fields.^{12,13} In this system, the observed magnetization consists of intergranular magnetic moments due to intergranular Josephson current and intragranular magnetic moments due to currents circulating in grains, and the intergranular magnetic moments give a major contribution to the total magnetization. Owing to the demagnetizing field by the intragrain magnetization, the internal field at the grain boundaries is effectively reduced. This allows the intergranular Josephson junction to cause a large Josephson current flow across the grain boundaries even at a positive field, resulting in a positive central peak position in this granular superconductor. As the temperature decreases, the central peak shifts toward a positive higher field owing to the increase in the demagnetizing field by increasing the number of trapped flux within the grains. This mechanism is different from our case that the stray field is independent of temperature due to a high Curie temperature of the magnetic Co moments and the central peak position strongly depends on the degree of field penetration into the superconducting film.

IV. SUMMARY

The influence of the ferromagnet magnetization on the magnetization hysteresis loops has been investigated on rf-sputtered ferromagnet(Co)/superconductor(Nb)/ferromagnet(Co) trilayered films under applied fields parallel

to the film surface. From our measurements, it is clear that when the ferromagnetic layer has in-plane magnetization, the central peak of the superconducting magnetization of F/S/F trilayers is shifted toward a positive field on the descending branch of the hysteresis loop. This is attributed to the fact that the stray field of the ferromagnet which is antiparallel to the in-plane magnetization effectively reduces the internal field of the superconductor and the condition that the mean internal field minimizes is achieved at a positive applied field. This observation is in contrast to the behavior of a single superconducting film where the central magnetization peak always shows up at zero field or at a slightly negative field.

For F/S/F-trilayered films the main effect of the in-plane magnetization is to shift the field position that the internal field of the superconductor minimizes. As a consequence, the position of the maximum critical current is shifted from zero applied field to a finite applied field.¹¹ Thus F/S/F trilayers may be applicable to a superconducting device where a maximum critical current is needed at a desired field.

ACKNOWLEDGMENT

We would like to thank Y. Kanno for his assistance with magnetization measurements.

*Present address: Institute of Multidisciplinary Research for Advanced Materials, Tohoku University, Sendai 980-8577, Japan.

¹G. Stejic, A. Gurevich, E. Kadyrov, D. Christen, R. Joynt, and D.C. Larbalestier, *Phys. Rev. B* **49**, 1274 (1994).

²A. Terentiev, D.B. Watkins, L.E. De Long, D.J. Morgan, and J.B. Ketterson, *Physica C* **324**, 1 (1999).

³V.T. Petrashov, I.A. Sosnin, I. Cox, A. Parsons, and C. Troadec, *Phys. Rev. Lett.* **83**, 3281 (1999).

⁴J. Aumentado and V. Chandrasekhar, *Phys. Rev. B* **64**, 054505 (2001).

⁵R.M. Osgood III, J.E. Pearson, C.H. Sowers, and S.D. Bader, *J. Appl. Phys.* **84**, 940 (1998).

⁶S.F. Lee, Y. Liou, Y.D. Yao, W.T. Shih, and C. Yu, *J. Appl. Phys.* **87**, 5564 (2000).

⁷M. Takeda and Y. Endoh, *Physica B* **267-268**, 185 (1999).

⁸S.V. Dubonos, A.K. Geim, K.S. Novoselov, and I.V. Grigorieva, *Phys. Rev. B* **65**, 220513 (2002).

⁹D.-X. Chen and R.B. Goldfarb, *J. Appl. Phys.* **66**, 2489 (1989).

¹⁰M. Däumling and W. Goldacker, *Z. Phys. B: Condens. Matter* **102**, 331 (1997).

¹¹S. Kobayashi, Y. Kanno, and F. Itoh, *Physica B* (to be published).

¹²K.-H. Müller, C. Andrikidis, and Y.C. Guo, *Phys. Rev. B* **55**, 630 (1997).

¹³M.R. Koblischka, L. Püst, A. Galkin, and P. Nálezka, *Appl. Phys. Lett.* **70**, 514 (1997); D.V. Shantsev, M.R. Koblischka, Y.M. Galperin, T.H. Johansen, L. Püst, and M. Jirsa, *Phys. Rev. Lett.* **82**, 2947 (1999).